Reduction of Flavins by Thiols. 3. The Case for Concerted *N,S*-Acetal Formation in Attack and an Early Transition State in Breakdown[1]

Edward L. Loechler*† and Thomas C. Hollocher*

Contribution from the Department of Biochemistry, Brandeis University, Waltham, Massachusetts 02254. *Received November 28, 1979*

Abstract: In the attack of dithiothreitol (DTT) monoanion at flavin C(4a) to form the intermediate *N,S*-acetal, α for general-acid catalysis at N(5) was determined to be 0.58, 0.49, and 0.34 for 3-methyl- (**3**), 7-chloro- (**4**), and 7,8-dichlororiboflavin (**6**), respectively. Thus $-(\partial\alpha/\partial\sigma) = p_{xy}' = 0.29$. Because Brønsted plots were linear for these flavins, $\partial\alpha/\partial pK_{HA} = p_x = 0$. Linear Hammett plots were observed for hydronium ion ($\rho = 0.1$) and water ($\rho = 3.24$) in the general-acid-catalyzed attack step, in the breakdown of the *N,S*-acetal ($\rho = 3.21$) and for flavin E_0' values ($\rho = 4.64$). In assigning σ values substituents at C(7) and C(8) of flavin were taken to be meta and para, respectively, with regard to the reaction center at N(5) and C(4a). With other general acids, including acetic acid, phosphate monoanion and glycine ethyl ester, Hammett plots for attack showed upward curvature and $-(\partial\rho/\partial\sigma) = p_y' = -3.6$. It is shown that preassociation hydrogen-bonding pathways involving the species $T^-\cdot HA$ and $FlH^+\cdot A^-$ cannot account for the observed general-acid-catalyzed rates. The attack step thus appears to be truly concerted, with proton transfer and S–C–N bond rearrangements occurring simultaneously. With use of the treatment proposed by Jencks and Jencks[4] for reaction coordinate diagrams and the structure-reactivity parameters p_x, p_y', and p_{xy}', the transition state for the glycine ethyl ester assisted addition of DTT to **4** occurs at $\alpha = 0.49$ and $\rho_n = 0.41$ with level lines of 0° and 134° at the transition state. The minimum energy path (reaction coordinate) through the transition state bisects the level lines and has a slope of 0.41 with respect to the $x' = \alpha$ axis of a transformed reaction diagram. This result also implies concerted general-acid catalysis in attack. Structure-reactivity effects for breakdown of the *N,S*-acetal suggest an early transition state with little S–S bond formation or C–S bond breakage. The effective molarity of 53 M for DTT compared with mercaptoethanol implies that some entropy must be lost in this early transition-state reaction. In Appendix I the pK for **3** protonated at N(5) was estimated to be −6.6.

Introduction

In the preceding two papers[2,3] the dithiol–flavin reaction was demonstrated to occur in three steps (Scheme I of the first paper in this series[2]): general-acid-catalyzed thiolate attack at flavin C(4a) to form an adduct (*N,S*-acetal), general-base-catalyzed deprotonation of the –SH group of the adduct, and uncatalyzed breakdown by reaction of the resulting thiolate. This paper considers structure-reactivity effects on the attack and breakdown steps when the flavin is modified.

Experimental Section

Materials, procedures, and kinetic treatment were as described in the first paper of this series.[2] The treatment of Jencks and Jencks[4] for reaction coordinate diagrams was applied to our data as described for class e reactions, of which general-acid-catalyzed attack of thiolate on flavin is an example.

Results

Reaction of 4 and 6 with DTT.[5] The kinetics was qualitatively similar to those for the reaction of **3** with dithiothreitol (DTT).[2] Buffer catalysis was observed to level off with increasing [buffer], and the data were fit by eq 1 of the first paper.[2,6] The pH rate profiles for the solvent terms are shown in Figure 1 for these flavins. The breakdown rate constants (k_B, open symbols) appear first order in hydroxide ion in this pH range, below pK_1 of DTT. At these pH values the fraction of dianionic DTT is negligible, and the solvent attack rate constants (k_A, solid symbols) can be fit by eq 1.

$$k_A = k_{a0} + k_{a1}(K_1/a_H) \qquad (1)$$

Tables I and II summarize the results for buffer catalysis, expressed as general-acid-catalyzed attack of DTT monoanion on **4** and **6**, respectively. These data have been plotted in Brønsted plots (Figure 2) along with the results for **3**[2] for immediate comparison. The α values are 0.58, 0.49, and 0.34 for **3**, **4**, and **6**, respectively. Only the water point for **6** was excluded from the α determinations, because this point lies 1.5 log units below the best straight line for the other general acids.

Scheme I

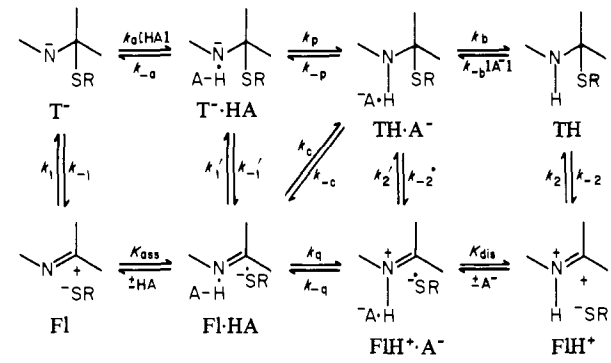

On the basis of the results in the preceding paper,[3] the calculated values for buffer-catalyzed *deprotonation* for **4** and **6** were greater than those for *attack* by at least 1 order of magnitude. Thus the deprotonation step was not kinetically significant for these two derivatives.

Hammett Plots. Figure 3 shows Hammett plots for the reaction of DTT monoanion with the three flavins and several general acids

(1) Supported by grants from the National Science Foundation (Grants GB-29337A1, PCM74-04834, PCM76-21678) and by a training grant from the National Institutes of Health (Grant GM-212). We thank John Lambooy, Peter Hemmerich and Franz Müller for the flavin derivatives used in this study. We also thank William Jencks for many useful discussions.

(2) Part I: Loechler, E. L.; Hollocher, T. C. *J. Am. Chem. Soc.*, accompanying paper in this issue.

(3) Part II: Loechler, E. L.; Hollocher, T. C. *J. Am. Chem. Soc.*, accompanying paper in this issue.

(4) Jencks, D. A.; Jencks, W. P. *J. Am. Chem. Soc.* **1977**, *99*, 7948.

(5) The structures of flavins **1** through **8** can be found or inferred in the first paper of this series.[2]

(6) In the reaction of **6** with DTT at pH 6.2, phosphate exhibited biphasic kinetics above 30 mM and was unique among the buffers studied. The initial slope in pseudo-first-order plots was less than the final slope. The rate constant associated with the initial slope was consistent with data obtained at [phosphate] < 30 mM. The special rate enhancement by phosphate would seem to be related to the appearance of reduced flavin as the reaction progressed. Only data from experiments where [phosphate] < 30 mM were used in calculations.

† Address correspondence to E.L.L. at the Biology Department, Massachusetts Institute of Technology, Cambridge, MA 02139.

0002-7863/80/1502-7328$01.00/0

Table I. General-Acid-Catalyzed Rate Constants for the Attack of DTT Monoanion on 4 at 25 °C and Ionic Strength 1.0 M (KCl)

general acid	pK^a	total buffer, M	pH	k_{AC}, M^{-2} min^{-1}	k_{ac_1},[c] M^{-2} min^{-1}
hydronium ion	−1.74				2.97×10^{9}[d]
acetic acid	4.59	0–0.200	6.99[b]	29.3	1.55×10^{6}
potassium phosphate	6.46	0.02–0.06	6.99	433	2.75×10^{5}
glycine ethyl ester hydrochloride	7.95	0.03–0.05	7.65	720	3.47×10^{4}
triethylenediamine hydrochloride	9.21	0.06–0.16	7.93	650	1.11×10^{4}
water	15.74				5.26[d]

[a] pK values as per Table I, first paper in this series[2]. [b] pH maintained with phosphate buffer. [c] $k_{ac_1} = k_{AC}/(F_{HSS^-}F_{HA})$. [d] Determined from the rate constants for the solvent reaction (Figure 1).

Table II. General-Acid-Catalyzed Rate Constants for the Attack of DTT Monoanion on 6 at 25 °C and Ionic Strength 1.0 M (KCl)

general acid	pK^a	total buffer, M	pH	k_{AC}, M^{-2} min^{-1}	k_{ac_1},[c] M^{-2} min^{-1}
hydronium ion	−1.74				2.70×10^{9}[d]
methoxyacetic acid	3.39	0.005–0.025	4.44	63.8	3.91×10^{7}
acetic acid	4.59	0.003–0.050	4.80	186	10.7×10^{6}
		0.004–0.050	5.65	248	9.58×10^{6}
piperizine hydrochloride	6.01[b]	0.002–0.060	5.60	1280	6.23×10^{6}
potassium phosphate	6.46	0.004–0.030	6.16	3440	4.94×10^{6}
imidazole hydrochloride	7.24	0.003–0.100	6.39	4100	2.62×10^{6}
glycine ethyl ester hydrochloride	7.95	0.002–0.025	7.00	8580	1.33×10^{6}
water	15.74				83.0[d]

[a] pK values as per Table I, first paper in this series[2]. [b] Reference 33. [c] $k_{ac_1} = k_{AC}/(F_{HSS^-}F_{HA})$. [d] Determined from the rate constants for the solvent reaction (Figure 1).

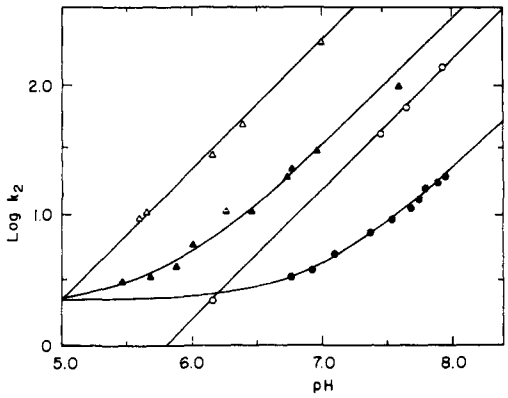

Figure 1. The pH rate profile for the attack step (k_A, solid symbols) and breakdown step (k_B, open symbols) in the reduction of **4** (circles) and **6** (triangles) by DTT at 25 °C and ionic strength 1.0 M (KCl). The pH-independent rate constants in attack are k_{a0} and k_{a1} and that in breakdown is k_{b1} with values, respectively, of 2.15, 292, and 2110 for **4** and 1.96, 4600, and 30800 for **6**. Units are M^{-1} min^{-1}.

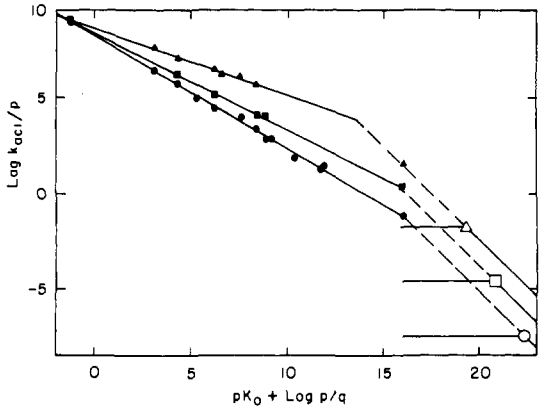

Figure 2. Brønsted plots for the general-acid-catalyzed attack of DTT monoanion of **6** (solid triangles), **4** (solid squares), and **3** (solid circles) at 25 °C and ionic strength 1.0 M (KCl). α is 0.34, 0.49, and 0.58, respectively. The solid lines of slopes 0 and −1 represent the calculated Eigen plots (see text) for general-acid-catalyzed trapping of the hypothetical intermediate, T^-. The dashed lines extend the out diffusion-trapping lines to the observed Brønsted lines. Units are M^{-2} min^{-1}.

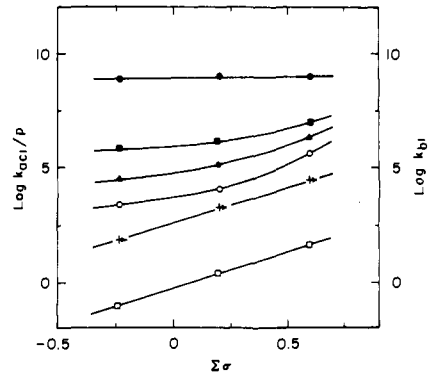

Figure 3. Hammett plots for the general-acid-catalyzed attack step (k_{ac1}, M^{-2} min^{-1}) and the breakdown step (k_{b1}, M^{-1} min^{-1}) in the reduction of **3**, **4**, and **6** by DTT at 25 °C and ionic strength 1.0 M (KCl). The general acids in attack (left ordinate) are hydronium ion (●), acetic acid (■), potassium phosphate (▲), glycine ethyl ester hydrochloride (○), and water (□, $\rho = 3.24$). ↔ refers to k_{b1} right orginate, $\rho = 3.21$. The σ assignments are −0.239 (7-CH_3, 8-CH_3) for **3**, +0.203 (7-Cl, 8-CH_3) for **4**, and +0.600 (7-Cl, 8-Cl) for **6**.

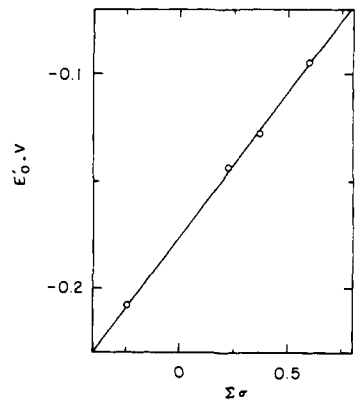

Figure 4. Dependence of E_0' on $\sum\sigma$ for several riboflavins with substituents at positions 7 and 8 in the benzene ring. The σ assignments are: −0.239 (7-CH_3, 8-CH_3), +0.227 (7-H, 8-Cl), +0.373 (7-Cl, 8-H), and +0.6 (7-Cl, 8-Cl). The E_0' values for the first three derivatives are from Walsh and co-workers,[28] while that for the last is from Kuhn and co-workers.[29] The slope of the line is +0.134 which, when converted to free energies, gives $\rho = 4.54$ for flavin reduction.

in attack and breakdown. The values of σ were determined by assuming that substituents at C(7) are meta ($\sigma_{CH_3} = -0.069$, $\sigma_{Cl} = +0.373$)[7] and at C(8) are para ($\sigma_{CH_3} = -0.17$, $\sigma_{Cl} = +0.227$)[7] and that σ values are additive. σ values so assigned gave linear

Table III. Summary of the Constants Used To Test the Reasonableness of the Preassociation Mechanisms through T^-·HA and FlH^+·A^- in the Attack of DTT Monoanion on Flavins with Glycine Ethyl Ester Hydrochloride as General Acid

flavin	log k_f,[a] M^{-1} s^{-1}	log K_{Add}[b]	α[c]	pK_{TH}[d]	log K_{AB}[e]	log k_r,[f] sec^{-1}	pK_{FlH^+}[g]	log K_{AB}'[e]	log k_x[h]	σ
3-methyllriboflavin (3)	2.07	−5.00	0.58	22.7	2.8	17.6	−6.6	3.5	13.1	−0.239
7-chlororiboflavin (4)	2.74	−3.67	0.49	20.9	2.4	15.4	−8.1	3.8	15.0	+0.203
7,8-dichlororiboflavin (6)	4.34	−2.47	0.34	19.3	2.1	14.5	−9.4	4.1	17.6	+0.600

[a] k_f was calculated from k_{ac_1} (Table II, first paper in this series[2]) and Tables I and II for glycine ethyl ester. [b] From Table IV, preceding paper[3]. [c] From Figure 2. [d] Estimated as outlined in Appendix I. [e] Estimated by using eq 3. [f] k_r is calculated from eq 2. [g] Estimated as outlined in Appendix I. [h] k_x is calculated from eq 4.

Scheme II

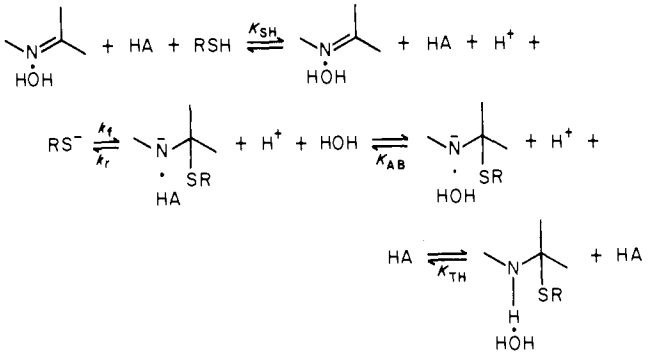

Scheme III

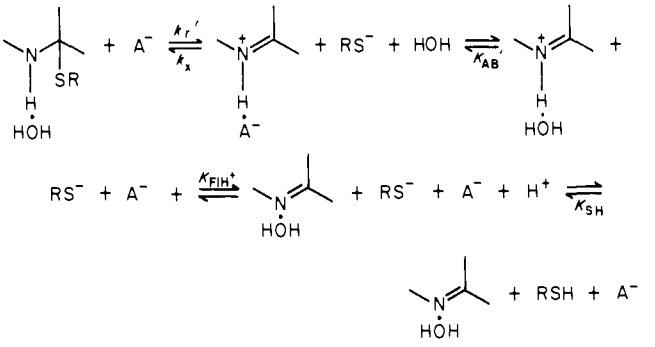

Hammett plots for k_{bl}, K_{Add} (preceding paper[3]), and E_0' of flavin (Figure 4). However reversal of the meta–para assignment or the use of σ^n or σ^+ values did not alter these plots significantly.

Straight lines through the data for breakdown (k_{bl} →) and for water and hydronium-catalyzed attack gave ρ values of 3.21, 3.24, and 0.1, respectively, in Figure 3. The data for the other general acids were connected by curved lines. No other combination of σ values (σ^n, σ^+, etc.) gave linear plots for these acids.

Discussion

Buffer Catalysis. The attack of thiols at flavin C(4a) leads to the formation of an *N,S*-acetal. Scheme I represents general reactions of this type.[8,9] Dots are used here and elsewhere to represent encounter complexes and not radical species. Buffer catalysis would be observed if steps k_a (trapping pathway), k_c (concerted pathway), and k_1' or k_2' (preassociation pathways) were rate determining. The preassociation pathway through step k_1' can be a hydrogen-bonding mechanism if hydrogen bonding by the general acid can stabilize developing negative charge. Inasmuch as the Brønsted plots of Figure 3 are not Eigen curves,[10] the trapping pathway through T^- can be precluded.

Precluding the Hydrogen-Bonding Mechanism through T^-·HA. A calculation of the reasonableness of this pathway can be made the basis of Scheme II. The overall equilibrium is K_{Add} and

$$k_r = \frac{k_f K_{SH}}{K_{Add} K_{AB} K_{TH}} \quad (2)$$

The observed rate constant for general-acid catalysis would be k_f. K_{TH} has been estimated for the three flavin derivatives (Appendix I). K_{AB} is the equilibrium constant for hydrogen bond formation in water between an acid (HA) and a base (B) and was estimated from the equation proposed by Hine[11] (eq 3). pK_{H_2O}

$$HA + B \overset{K_{AB}}{\rightleftharpoons} B{\cdot}HA$$

$$\log K_{AB} = \tau(pK_{HA} - pK_{H_2O})(pK_{H_3O^+} - pK_{HB}) - 1.74 \quad (3)$$

and $pK_{H_3O^+}$ were taken as +15.74 and −1.74, respectively, and τ was taken as 0.024 as proposed by Hine.[11,12] pK_{HA} and pK_{HB} in eq 3 represent the pK of the general acid (HA) and adduct (TH), respectively, in Scheme II. k_f (Tables I and II), pK_{SH} (9.14), and K_{Add}[3] are known.

Values of k_r for the three flavins (Table III) with glycine ethyl ester as general acid lie in the range 10^{14}–10^{18} s^{-1} and so are larger than the fastest possible rate constant in water (out difussion ≈ 10^{11} s^{-1}).[10] We conclude that attack is faster than that permitted by this hydrogen-bonding mechanism.

Precluding the Preassociation Pathway through FlH_A^+. The reasonableness of this mechanism can be tested by calculations based on Scheme III, where the overall equilibrium is K_{Add}^{-1}. Because k_r' (the observed general-base-catalyzed rate constant for the reverse reaction) is related to the observed forward general-acid-catalyzed rate constant k_f by $k_r' = (k_f K_{SH}/K_{Add}K_{HA})$, eq 4 can be derived. k_f and K_{HA} are known, while K_{AB}' was

$$k_x = \frac{k_f K_{FlH^+}}{K_{HA} K_{AB}'} \quad (4)$$

estimated from the Hine equation[11] and K_{FlH^+} was estimated as outlined in Appendix I. These values are tabulated in Table III with glycine ethyl ester as general acid. The values for k_x (10^{13}–10^{18} s^{-1}) preclude a preassociation mechanism involving FlH^+·A^-.

Reaction Coordinate Diagram. Hammett plots showed upward curvature with increasing σ for attack catalyzed by acetic acid, phosphate monoanion, and glycine ethyl ester (Figure 3) but were linear for adduct formation,[3] breakdown, water- and hydronium-catalyzed attack, and E_0' (Figure 4). These linear curves suggest that σ values were correctly assigned and that the curvature observed with the three buffers is real. With use of the method of Jencks and Jencks[4] the transition state and its level lines can be located on the transformed reaction diagram of Figure 5A for thiol addition to flavin. Linear Brønsted plots (Figure 2) gave $\partial\alpha/\partial pK_{HA} = p_x = 0$. The Hammett plots gave $-(\partial\rho/\partial\sigma) = p_y'$ $= -3.6$,[14] and a plot of α vs. σ gave $-(\partial\alpha/\partial\sigma) = p_{xy}' = 0.29$.[15] p_y'

(7) Exner, O. "Advances in Free Energy Relationships"; Chapman, N. B., Shorter, J. Eds.; Plenum Press: New York, 1972; p 1.
(8) Gilbert, H. F.; Jencks, W. P. *J. Am. Chem. Soc.* **1977**, *99*, 7931.
(9) Jencks, W. P. *Acc. Chem. Res.* **1976**, *9*, 425.
(10) Eigen, M. *Angew. Chem., Int. Ed. Engl.* **1964**, *3*, 1.
(11) Hine, J. *J. Am. Chem. Soc.* **1971**, *93*, 3701.
(12) See discussion of τ in footnote 26 of ref 13.
(13) Funderburk, L. H.; Jencks, W. P. *J. Am. Chem. Soc.* **1978**, *100*, 6708.
(14) The values for $-p_y'$ were 4.4, 3.5, 2.9, and 0.0 for glycine ethyl ester, phosphate monoanion, acetic acid, and hydronium ion, respectively. The average of the first three gave $p_y' = -3.6$. The results for hydronium ion are discussed in the text. Curved Hammett plots are not required in order to apply the treatment of Jencks and Jencks.[4] Straight lines conceivably could be drawn through the data of Figure 3 to give $p_y' = 0$. The slopes of the level lines in Figure 5A would then become 0 and ∞ relative to the y' axis and the bisector angle a' would become 45°. This value is also consistent with a concerted process.

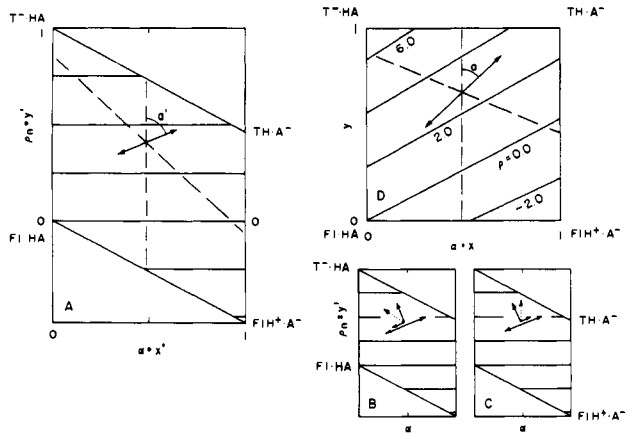

Figure 5. (A) Transformed reaction coordinate diagram for glycine ethyl ester catalyzed addition of DTT monoanion to **4**. The horizontal and vertical coordinates are, respectively, observed α and $\rho_n = \rho/\rho_{eq}$ where ρ_{eq} is the difference in ρ between the top and bottom of the figure. The difference in ρ between the two left corners at $\alpha = 0$ is 7.09 and that between the two right corners at $\alpha = 1$ is 6.45.[16] Thus $\rho_{eq} = 7.09 - 0.64\alpha$. Level lines (dashed) intersect at the transition state ($\alpha = 0.49$ and $\rho_n = 0.41$).[4] The bisector of the level lines (double arrow) is taken to be the reaction coordinate. α represents the extent of proton transfer, and ρ_n represents the extent of covalent reaction at N(5). (B) Transformed reaction coordinate diagram as in A showing the vectors (solid) and resultant (dotted) for displacement of the transition state as σ is increased. Increasing σ raises (destabilizes) $FlH^+\cdot A^-$ and lowers $T^-\cdot HA$ and $TH\cdot A^-$. (C) Transformed reaction coordinate diagram like B but showing the displacement of the transition state as pK_{HA} is increased. Increasing pK_{HA} lowers Fl·HA and $T^-\cdot HA$ equally with the result that no displacement occurs along α. (D) Orthogonal reaction coordinate diagram calculated from A. Extent of reaction at N(5) as measured by ρ is indicated by the diagonal lines. The vertical coordinate is defined by $y = (\rho + 3.43\alpha)/(7.09-0.64\alpha) \simeq \rho_n - 0.53\alpha$.

and p_{xy}' are divided by $\bar{\rho}_{eq}^2$ and $\bar{\rho}_{eq}$, respectively, to convert from an energy scale based on σ to one based on base 10 logarithms.[4,16] Normalized p_y' and p_{xy}' are −0.079 and 0.043, respectively. The level lines intersect at the transition state which has locus $\alpha = 0.49$ and $\rho_n = 0.41$ (or $\rho = 2.8$). Slopes of the level lines are 0 and −1.08[17] relative to the y' axis with an angle of 134° between them. The bisector of the level lines represents the calculated minimum energy path to the transition state, and we take this path to be the reaction coordinate. Relative to the x' axis, the bisector has the slope

$$\frac{p_y' + \sqrt{p_y'^2 + (2p_{xy}')^2}}{2p_{xy}'} = 0.41$$

which defines an angle a' of 67°.[18] This angle and the previous finding[2] that $\beta_{nuc} = 0.55$ for DTT addition to **3** are consistent with concerted catalysis.

The curvature parameters are $a' = -21$, $b' = 0$, and $c' = -23$.[17] A negative value of $a' = -12$ was also reported for the class e general-base-catalyzed reaction of water and alcohols with formaldehyde.[19]

With increasing σ the transition state is expected to move parallel (Hammond effect)[20] and perpendicular (anti-Hammond effect)[21] to the original transition state as indicated in Figure 5B. The resultant cuts across isoρ lines, as required by the observed increase in ρ with σ.

It is customary to convert transform diagrams to orthogonal coordinates for ease of viewing, and this is done in Figure 5D. The level lines now subtend angles of 0 and 112° from the vertical, and the reaction coordinate subtends an angle a of 47°.[22]

Movement of the Transition State with Changes in General Acid pK. The proton points of Figure 4 show a very low ρ value (+0.1), indicating that the charge at N(5) in the transition state is about what it is in reactants. Thus these points lie on or near the line of $\rho = 0$ in Figure 5A. The rate constants for proton catalysis are remarkably large ($\sim 3 \times 10^7$ M^{-2} s^{-1}). The rate constant for the DTT monoanion reaction with the flavin-proton encounter complex ($K_e \approx 10^{-1}$ M^{-1}) would be 3×10^8 M^{-1} s^{-1} which can be compared with a rate constant of 5×10^7 M^{-1} s^{-1} for the reaction of hydroxide ion at C(4a) of 3,5-dimethyllumiflavonium ion.[23]

As the general acid becomes weaker, the left edge of the reaction coordinate diagram (Figure 5C) must become lower and cause a displacement of the transition state toward the top edge of the diagram (larger ρ). The prediction that ρ should increase with weaker acids is confirmed in Figure 3.

Mechanism with Water as General Acid. The water points do not show the upward curvature in Figure 3 observed for the other general acids. For an explanation consider the reverse of water-assisted attack, namely hydroxide-assisted breakdown of TH, step k_{-a1} in Scheme IV, where

Scheme IV

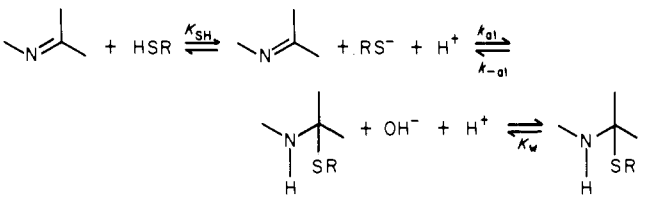

Scheme V

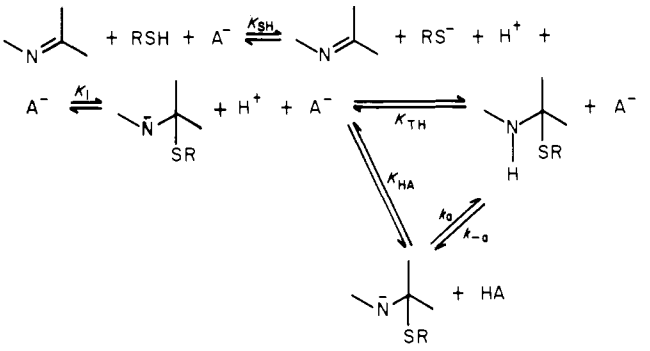

(15) $\partial\rho/\partial pK_{HA}$ also equals p_{xy}'. Plots of ρ vs. pK_{HA} gave slopes of 0.17, 0.29, and 0.53 for **3**, **4**, and **6**, respectively, for an average p_{xy}' of 0.33. Plots of $-p_y'$ vs. pK_{HA} and p_{xy}' vs. σ (slope $= \partial\rho/\partial\sigma\partial pK_{HA}$ in each case) gave straight lines with slope 0.46. Variable p_{xy}' and p_y' values may have resulted from the limited number of compounds studied or experimental error. However, it also may have resulted from the large area sampled on the reaction coordinate diagram with α ranging between 0.34 and 0.58 and ρ between 0.0 and 5.0. This area may exceed that for which the equations proposed by Jencks and Jencks[4] strictly hold.

(16) ρ_{Add} in Fl → TH is 3.02.[3] ρ for ionization of TH is taken to be 4.07, which is the value for ionization of aniline and dibenzylamine.[40] Thus in Fl → T^-, $\rho = 7.09$. Ionization of FlH^+ is analogous to ionization of *N,N*-dimethylanilinium for which $\rho = 3.43$.[44] Thus the corner ρ values in Figure 5 are 0, 7.09, 3.02, and −3.43 for Fl·HA, $T^-\cdot HA$, $TH\cdot A^-$, and $FlH^+\cdot A^-$, respectively. ρ_{eq} is defined in the legend to Figure 5. The average value of ρ_{eq} is $\bar{\rho}_{eq} = 6.77$ and is simply the average difference in ρ between the two left corners and the two right corners. Given the corner values of ρ, the relationship $\rho = 7.09y - 3.43x - 0.64xy$ applies to Figure 5D where x and y vary between 0 and 1.

(17) When $p_x = 0$, the curvature parameters for the transformed diagram are a function of normalized p_y' and p_{xy}': $a' = p_y'/2p_{xy}'^2$, $b' = 0$, and $c' = -1/p_{xy}'$. The slopes of the level lines relative to the y' axis are 0 and $-c'/a' = 2p_{xy}'/p_y'$.

(18) This expression for bisector slope applied when $p_x = 0$.

(19) Funderburk, L. H.; Aldwin, L.; Jencks, W. P. *J. Am. Chem. Soc.* **1978**, *100*, 5444.

(20) Leffler, J. E. *Science (Washington, D.C.)* **1953**, *117*, 340. Hammond, G. S. *J. Am. Chem. Soc.* **1955**, *77*, 334.

(21) Thornton, E. R. *J. Am. Chem. Soc.* **1967**, *89*, 2915.

(22) In Figure 5A the 134° level line defines the line $\rho_n = -0.92\alpha + 0.86$, while the bisector defines the line $\rho_n = 0.41\alpha + 0.21$. In Figure 5D these lines become $y = -0.39\alpha + 0.86$ and $y = 0.94\alpha + 0.21$, respectively, with the transition state at $\alpha = 0.49$ and $y = 0.66$. These functions were derived from the equation of ref 16.

(23) Kemal, C.; Bruice, T. C. *J. Am. Chem . Soc.* **1976**, *98*, 3955.

$$k_{-al} = \frac{k_{al}K_{SH}}{K_wK_{Add}} \quad (5)$$

Values for k_{-al} are 1.3, 1.6, and 1.6×10^9 M^{-1} s^{-1} for **3**, **4**, and **6**, respectively. These values are similar and are only 5–10 times lower than the diffusion-controlled reaction of hydroxide ion with an unchanged species ($\sim 10^{10}$ M^{-1} s^{-1}).[10] The magnitude of k_{-al} and its insensitivity to substituent effects suggest that the reaction may be partly diffusion controlled. Abnormally low diffusion-controlled rate constants have been observed and often attributed to steric hindrance of proton transfer.[24] This is likely to apply at the crowded N(5) region of TH.[55] It is likely therefore that the water points in Figure 3 fail to show curvature because k_b and not k_c of Scheme I is rate determining. If k_{-al} is not diffusion controlled, it must otherwise represent some rapid event which is not readily influenced inductively by polar substituents. This could be solvent rearrangement or an entropy effect wherein reactants in the encounter complex react rapidly when properly oriented but have a probability <1 of being so oriented.

Partial diffusion control of k_{-al} and the fact that the point for water-assisted attack on **6** lies 1.5 log units below the Brønsted line (Figure 2) suggest that k_{acl} is breaking from a concerted to an out diffusion step in the case of extremely weak general acids. The location of the out diffusion lines of slope −1 in Figure 2 were established by considering the trapping pathway through T^- of Scheme I. Eigen curves for this mechanism can be calculated from Scheme V. From the lower path an expression for the trapping rate constant can be derived

$$k_t = k_aK_1 = k_{-a}K_{HA}K_{Add}/K_{SH} \quad (6)$$

and because $k_aK_{TH} = k_{-a}K_{HA}$

$$k_t = k_aK_{TH}K_{Add}/K_{SH} \quad (7)$$

When k_a is diffusion controlled (10^9 M^{-1} s^{-1} when $pK_{HA} < pK_{TH}$), eq 7 can be used to construct the trapping curve of slope zero. When k_{-a} is diffusion controlled ($pK_{HA} > pK_{TH}$), eq 6 can be used to construct the curve of slope −1. The large open circle, the square, and the triangle of Figure 2 lie at the intersection of the lines of slope 0 and −1 for the trapping curves for **3**, **4**, and **6**, respectively. Dashed lines connect the Brønsted lines with the out diffusion lines of the trapping curve. While these trapping curves cannot be experimentally determined in water, they depend on observed kinetic parameters and pK_{TH} which can be estimated. Thus the positions of the "Eigen curves" are reliably placed. Beyond the point where the Brønsted line intersects the out diffusion line, the rate-determining step must change to diffusion,[25] as appears to be the case for water as general acid in attack of DTT on **6**. Breaks of this kind in Brønsted plots were predicted by Sayer and Jencks[25] and have been observed for the concerted general-base-catalyzed methoxyaminolysis of acetyltriazole.[26]

The vertical distances between the line of zero slope for the trapping curves of Figure 2 and the intersection of the observed Brønsted slopes with the dashed lines are 6.4, 5.1, and 5.6 log units for **3**, **4**, and **6**, respectively. This distance is much greater than that for a similar reaction, general-acid-catalyzed hemithioacetal formation,[8] which is one of the best documented examples of a hydrogen-bonding mechanism. These results can be rationalized by Figure 6. Curves 1 and 2 represent addition of methyl mercaptoacetate anion ($pK = 7.83$)[8] and pentafluorothiophenolate

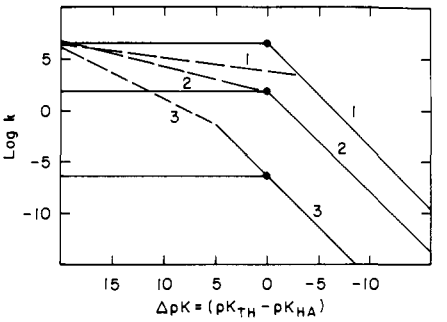

Figure 6. Dependence of the Brønsted plots for several thiol addition reactions on log K_1: trapping mechanisms, solid lines; hydrogen bonding or concerted mechanisms, dashed lines. Data points are omitted for clarity. For the addition of methyl mercaptoacetate anion to acetaldehyde (curve 1, log $K_1 = -2.4$) both trapping and hydrogen bonding ($\alpha = 0.13$) mechanisms were observed. For the addition of pentafluorothiophenolate to acetaldehyde (curve 2, log $K_1 = -7.4$) the trapping mechanism was observed below $\Delta pK = 0$, while the hydrogen bonding mechanism ($\alpha = 0.26$) was observed above $\Delta pK = 0$. For the addition of DTT monoanion to **4** (curve 3, log $K_1 = -15.6$) the concerted mechanism was observed ($\alpha = 0.49$). The position of the trapping mechanism in this reaction was calculated from eq 6 and 7. Data for addition to acetaldehyde were taken from Gilbert and Jencks.[8]

($pK = 2.68$)[8] to acetaldehyde, respectively, while curve 3 represents addition of DTT monoanion to **4**. Within this series the trapping curves (solid) decrease due to decreasing K_1 (destabilization of T^-) (eq 8). K_1 is decreased either by lowering the basicity of the

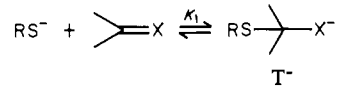

(8)

nucleophile or by increasing the pK at the heteroatom, X, of the adduct. In contrast the hydrogen bonding and concerted portions of the Brønsted plots (dashed) decrease to a smaller degree, because in these transition states there is less charge development on the heteroatom and less C–S bond formation

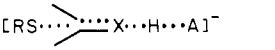

than for the trapping mechanism. When T^- is moderately stable the trapping mechanism predominates, but as T^- becomes increasingly unstable, the hydrogen-bonding and concerted pathways eventually predominate. This result also was anticipated by Sayer and Jencks,[25] although represented somewhat differently.

Structure-Reactivity Effects in the Breakdown Reaction. k_{12} and k_{-12} are evaluated in Appendix II (see eq 9). $k_{12} = 1.26$,

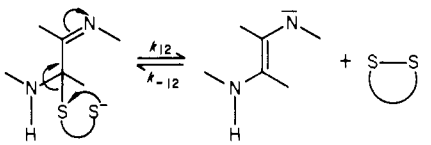

(9)

1.91, and 1.82×10^7 min^{-1} for **3**, **4**, and **6**, respectively, with DTT. The analogous constant, k_{12}^{ME}, is 2.4×10^5 M^{-1} min^{-1} for reaction of ME with **3**. The effective molarity is thus 53 M for DTT. $k_{-12} = 3.7$ and 0.27×10^{-5} M^{-1} min^{-1} and $K_{12} = k_{12}/k_{-12} = 0.34$ and 6.8×10^{12} M for **3** and **6**, respectively, with DTT. $k_{-12}^{ME} = 2.8 \times 10^{-5}$ M^{-1} min^{-1} for **3** and $K_{12}^{ME} = 8.5 \times 10^9$.

An approximate value of $\beta_S = 1.7$ at sulfur for the k_{-12} step can be estimated from k_{-12}^{ME} above and the reaction of reduced **3** with DTNB ($k_{rl} = 1.8 \times 10^4$ M^{-1} min^{-1}, first paper of this series[2]). This indicates that both sulfur atoms of the disulfide have picked up nearly a full negative charge in the transition state and compares well with cyanide ion attack on aromatic disulfides, where $\rho = 4.18$[30] ($\beta_S = 2.25$, if ρ for thiophenol ionization is 1.86).[31]

(24) Bernasconi, C. F.; Carré, P. *J. Am. Chem. Soc.* **1979**, *101*, 2698, 2707. Crooks, J. E. "Proton Transfer Reactions", Caldwin, E., Gold, V., Eds.; Wiley: New York, 1975; p 153. Caldwin, E. F.; Crooks, J. E.; O'Donnell, D. *J. Chem. Soc., Faraday Trans. 1* **1973**, *69*, 993. Caldwin, E. F.; Crooks, J. E. *J. Chem. Soc. B* **1967**, 959. Ralph, E. K.; Grunwald, E. *J. Am. Chem. Soc.* **1967**, *89*, 2963.

(25) Sayer, J. M.; Jencks, W. P. *J. Am. Chem. Soc.* **1973**, *95*, 5637; **1974**, *96*, 7998.

(26) Fox, J. P.; Jencks, W. P. *J. Am. Chem. Soc.* **1974**, *96*, 1436.

(27) Zahler, W. L.; Cleland, W. W. *J. Biol. Chem.* **1968**, *243*, 716.

(28) Walsh, C.; Fisher, J.; Spencer, R.; Graham, D. W.; Ashton, W. T.; Brown, J. E.; Brown, R. D.; Rogers, E. F. *Biochemistry* **1978**, *17*, 1942.

(29) Kuhn, R.; Weygand, F.; Friedrich, E. *Chem. Ber.* **1943**, *76*, 1044.

(30) Happer, D. A. R.; Mitchell, J. W.; Wright, G. J. *Aust. J. Chem.* **1973**, *26*, 121.

Scheme VI

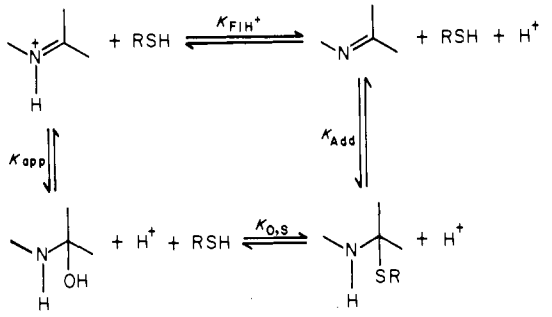

$$K_{FlH^+} = \frac{K_{app}K_{O,S}}{K_{Add}}$$

The slope of the line in Figure 4 is +0.134 and yields $\rho = 4.64$, after correction for N(1) ionization of reduced flavin, for the overall reduction of flavins. Given $\rho = 3.02$[3] for adduct formation, ρ for the k_{12} step is 1.6. This ρ value must result from the loss of the electron-withdrawing sulfur from the adduct, as well as the increase of one negative charge at N(1) in reduced flavin.

Several observations indicate that step k_{12} has an early transition state: (a) k_{12} is rather insensitive to substituents in the flavin benzene ring; (b) the monothiols, ME (pK = 9.61) and 3-mercaptopropionate (pK = 10.23), had similar values for the breakdown constant k_{MM};[3] because K_{Add} values are not expected to change with thiol pK,[8,32] the k_{12} values for both monothiols must be similar and thus β at sulfur must be small; (c) the back-reaction shows a large substituent effect at sulfur ($\beta_S \approx 1.7$), indicating a late transition state in this direction; (d) the step is thermodynamically favorable ($K_{12} \approx 10^{12}$ M). The observed EM = 53 M for DTT compared to ME implies that some entropy must be lost even in a reaction with an early transition state.

Appendix I

A. pK at N(5) for the DTT Adduct with 3. The method used to obtain $pK_{TH_2^+}$ is similar to that used by Sayer et al.[34] The pK of the indole adduct **5′** protonated at N(5) was reported as 4.4,[35] and lies within the range (4.3–5.5) expected for this kind of anilinium.[36,43] The difference in pK between **5′** and **6′** is

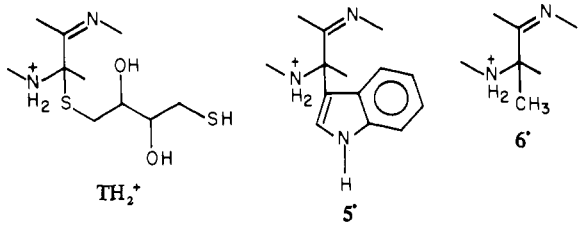

TH_2^+ **5′** **6′**

expected to be similar to that between the amino groups of tryptophan (pK = 9.39) and alanine (pK = 9.69).[37] Thus $pK_{6'} \simeq 4.7$. The pK of the hemithioacetal between acetaldehyde and ME is 12.4[8] while the pK of ethanol is 16.0,[38] a difference of 3.6 units. We therefore assume that $pK_{TH_2^+} \simeq pK_{6'} - 3.6 \simeq 1.1$.

Dolman and Stewart[39] found among diphenylamines that $pK_{NH} = 21.4 + 1.3pK_{NH_2^+}$. Thus $pK_{TH} \simeq 22.7$. Walba and Ruiz-Velasco[40] developed a similar relationship for benzimidazoles from which $pK_{TH} \simeq 24.3$. We favor the former value, because TH is more similar to diphenylamine than benzimidazole.

Scheme VII

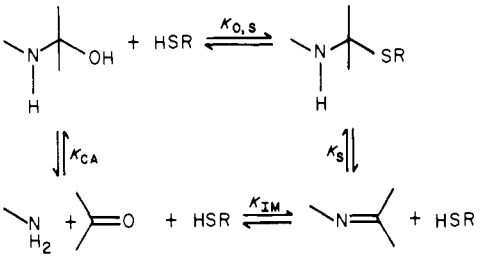

$$K_{O,S} = \frac{K_{IM}K_S}{K_{CA}}$$

B. pK at N(5) for the DTT Adduct of 4 and 6. For this the σ values listed under Results for Cl and CH_3 meta and para to N(5) were used so that $\sum\sigma$ for **3**, **4**, and **6** is −0.239, 0.203, and 0.600, respectively. ρ for ionization is about 2.8 for anilinium,[7,41,42] 3.36 for *N*-methylanilinium,[42] 3.43 for *N*,*N*-dimethylanilinium,[43] and 2.23 for phenol.[7] Dolman and Stewart[39] reported $\rho = 3.36$ and 4.07 for protonated and neutral diphenylamines, respectively, and $\rho \simeq 3.33$ and 4.07 can be inferred for anilinium and aniline, respectively, from their data. Taking $\rho = 4.07$ as appropriate

$$pK_{TH} = pK_{TH3} - 4.07(\sigma + 0.239)$$

Thus $pK_{TH} \simeq 20.9$ and 19.3 for **4** and **6**, respectively.

C. pK of 3 Protonated at N(5). pK_{FlH^+} can be estimated from a thermodynamic cycle (Scheme VI).

K_{app}. Kermal and Bruice[23] reported an apparent pK = 4.15 for the addition of hydroxide to C(4a) of 3,5,7,8,10-pentamethyllumiflavonium ion. In going from FlH^+ to the DTT adduct (from upper left to lower right in above cycle), the ρ change is about 6.4 (see text and ref 16) which corresponds to a decrease in positive charge at N(5) of between 1 and 2 (ca. 1.5). We expect a similar change in charge upon addition of hydroxide to N(5) alkyl flavonium ions. For this reaction ρ^* at N(5) is taken to be 1.5ρ for ionization of protonated tertiary amines:[44] $\rho^* \simeq 1.5 \times 3.3 \simeq 5$. Because $\sigma_H^* = 0.49$,[45] $pK_{app} \simeq 4.15 - \rho^*\sigma_H^* \simeq 1.7$ with an uncertainty of about ± 1.0.

$K_{O,S}$. There has been no direct comparison of the stability of *N*,*S*-acetals with their corresponding carbinolamines. The thermodynamic cycle (Scheme VII) was used to estimate $K_{O,S}$. Sayer[46] found $K_S = 18$ M^{-1} for the addition of mercaptoethanol to the imine, *N*-(*p*-chlorobenzylidine)aniline. Cordes and Jencks[47] obtained a value of $K_{IM} = 4.6$ M^{-1} for *N*-(*p*-chlorobenzylidene)aniline formation from aniline and *p*-chlorobenzaldehyde. K_{CA} has not been measured for the adduct between aniline and *p*-chlorobenzaldehyde, but a reliable estimate can be made. Abrams and Kallen[42] reported a value of 22.3 M^{-1} for the formation of carbinolamine from aniline and formaldehyde hydrate. Sanders and Jencks[48] have demonstrated a relationship between adduct formation for various nucleophiles and carbonyls, including *p*-chlorobenzaldehyde and formaldehyde. If this relationship holds for aniline, it should add to *p*-chlorobenzaldehyde 4.3×10^6 times as poorly as to formaldehyde or with use of the value of formaldehyde hydration used by Sanders and Jencks ($K_{hyd} = 2270$)[49] 1.89×10^3 times as poorly as to formaldehyde hydrate. Thus K_{CA} should be about 1.18×10^{-2} M^{-1} (22.3 M^{-1}/1.89×10^3). This value can be compared to the value of 4×10^{-2} M^{-1} for

(31) See footnote 47 of ref 2.
(32) Kanchuger, M. S.; Byers, L. D. *J. Am. Chem. Soc.* **1979**, *101*, 3005.
(33) Gravitz, N.; Jencks, W. P. *J. Am. Chem. Soc.* **1974**, *96*, 489.
(34) Sayer, J. M.; Peskin, M.; Jencks, W. P. *J. Am. Chem. Soc.* **1973**, *95*, 4277.
(35) Clerin, D.; Bruice, T. C. *J. Am. Chem. Soc.* **1974**, *96*, 5571.
(36) Brown, H. C.; McDaniel, D. H.; Häfliger, O. "Determination of Organic Structures by Physical Methods"; Braude, E. A.; Nachod, F. C., Eds.; Academic Press: New York, 1955; p 567.
(37) Dawson, R. M. C.; Elliot, D. C.; Elliot, W. H.; Jones, K. M. "Data for Biochemical Research", 2nd ed.; Oxford University Press: New York, 1969; p 430.
(38) Ballinger, D.; Long, F. A. *J. Am. Chem. Soc.* **1960**, *82*, 795.
(39) Dolman, D.; Stewart, R. *Can. J. Chem.* **1967**, *45*, 911; Stewart, R.; Dolman, D. *Ibid.* **1967**, *45*, 925.
(40) Walba, H.; Ruiz-Velasco, R. *J. Org. Chem.* **1969**, *34*, 3315.
(41) Biggs, A. I.; Robinson, R. A. *J. Chem. Soc.* **1961**, 388.
(42) Abrams, W. R.; Kallen, R. G. *J. Am. Chem. Soc.* **1976**, *98*, 7777.
(43) Fickling, M. M.; Fischer, A.; Mann, B. R.; Packer, J.; Vaughan, J. *J. Am. Chem. Soc.* **1959**, *81*, 4226.
(44) Hall, H. K. *J. Am. Chem. Soc.* **1957**, *79*, 5441.
(45) Hine, J. S. "Physical Organic Chemistry", 2nd ed.; McGraw-Hill: New York, 1962; p 97.
(46) Sayer, J. M., personal communication.
(47) Cordes, E. H.; Jencks, W. P. *J. Am. Chem. Soc.* **1962**, *84*, 826.
(48) Sanders, E. G.; Jencks, W. P. J. *Am. Chem. Soc.* **1968**, *90*, 6154.
(49) Via, F. A.; Hine, J. *J. Am. Chem. Soc.* **1972**, *94*, 190.

Scheme VIII

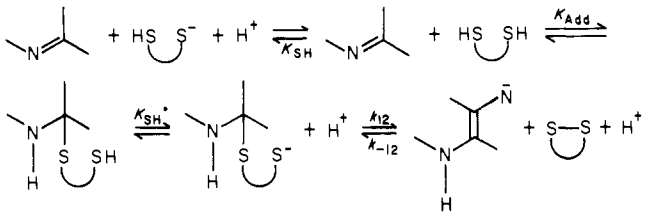

Scheme IX

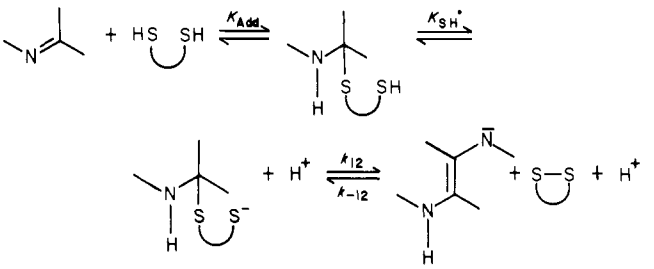

carbinolamine formation between isobutyraldehyde and trifluoroethylamine (pK = 5.22)[49] and 2 × 10^{-6} M^{-1} for addition of *p*-chlorobenzaldehyde and semicarbazide (pK = 3.86).[34] The latter constant is smaller because of the special stabilities of hydrazones. From the above,

$$\log K_{O,S} = \log K_{IM} + \log K_S - \log K_{CA} = 3.85$$

The equilibrium constant for hemithioacetal formation from acetaldehyde is independent of thiol pK,[8,32,50] and for many compounds the ratio of the equilibrium constants for addition of two different nucleophiles to carbonyls was shown to be constant.[48] Kanchuger and Byers[32] have shown that log $K_{O,S}$ = 3.2 and it is approximately constant for various aldehydes with the thiol, glutathione. log $K_{O,S}$ = 0.115 log K_S + 2.73 can be derived from their data.[32] With the assumption that it applies to imines as well as carbonyls, log $K_{O,S}$ = 2.1 for reaction of ME with **3**. On the basis of the above two values log $K_{O,S} \simeq 3.0 \pm 1.0$.

K_{Add}. K_{Add} for ME would be half that of DTT for statistical reasons. Thus log K_{Add} = −5.3.

From the above

$$pK_{FlH^+} = pK_{app} + \log K_{Add} - \log K_{O,S} \simeq -6.6\ (\pm 2.0)$$

This value is much lower than the observed p$K \approx 0$ for protonated oxidized flavin. The latter pK has been assigned to N(1) ionization (eq 10)[51]

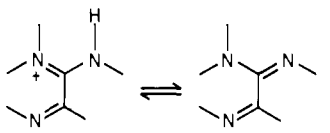

(10)

(50) Lienhard, G. E.; Jencks, W. P. *J. Am. Chem. Soc.* **1966**, *88*, 3982.

D. pK of 4 and 6 protonated at N(5). We assume that ρ for ionization at protonated N(5) is the same as for *N,N*-dimethylanilinium (ρ = 3.43).[43] With use of the $\sum\sigma$ values from *B* above and pK_{FlH^+} for **3** from C above, pK_{FlH^+} is −8.1 and −9.4 for **4** and **6**, respectively.

Appendix II. Structure-Reactivity Effects for the Breakdown Reaction

The rate constant for the breakdown step, k_{12}, in reactions of DTT can be calculated from Scheme VIII. The *observed* rate constant for breakdown, k_{b1}, is related to k_{12} by eq 11. k_{12} equals

$$k_{12} = \frac{k_{b1}K_{SH}}{K_{SH}'K_{Add}} \tag{11}$$

1.26, 1.91, and 1.82 × 10^7 min^{-1} for **3**, **4**, and **6**, respectively. K_{SH}/K_{SH}' is taken as 2 for statistical reasons. The analogous rate constant k_{12}^{ME} for the reaction of ME with **3** is 2.4 × 10^5 M^{-1} min^{-1}. This gives an effective molarity (EM) of 53 M for DTT.

The rate constant for the back-reaction with DTT, k_{-12}, can be estimated from Scheme IX. The overall equilibrium is K_{ov}, and at pH 7

$$K_{ov}' = \frac{[\text{red Fl}][\text{ox DTT}]}{[\text{Fl}][\text{DTT}]}$$

K_{ov}' can be determined from the E_0' values of −0.332,[27] −0.208,[28] and −0.095[29] V for DTT, riboflavin (assumed identical with **3**) and **6**, respectively. K_{ov}' is 1.6 × 10^4 and 1.1 × 10^8 for **3** and **6**, respectively. K_{ov} can be defined in terms of K_{ov}'

$$K_{ov} = \frac{K_{ov}'a_H}{(1 + a_H/K_{N(1)})}$$

where $K_{N(1)}$ is the ionization constant of reduced flavin at N(1)[28] and

$$k_{-12} = \frac{k_{12}K_{Add}K_{SH}'}{K_{ov}'a_H/(1 + a_H/K_{N(1)})} \tag{12}$$

k_{-12} is 3.7 × 10^{-5} and 0.27 × 10^{-5} M^{-1} min^{-1} and $K_{12} = k_{12}/k_{-12}$ = 0.34 × 10^{12} and 6.8 × 10^{12} M for **3** and **6**, respectively.

In an analogous manner k_{-12}^{ME} = 2.8 × 10^{-5} M^{-1} min^{-1} and K_{12}^{ME} = 8.5 × 10^9 for the reaction of **3** with ME, if E_0' of ME = −0.280 V. This E_0' value was estimated from the equilibrium constant (0.3 M^{-1})[52] for the reduction of 3-methyllumiflavin by ME at pH 10.86, where the E_0' value for 3-methyllumiflavin,[53] the pK of ME,[54] and the pK of reduced 3-methyllumiflavin at N(1)[51] were taken respectively to be −0.207 V, 9.61, and 6.6.

(51) Bruice, T. C. "Progress in Bioorganic Chemistry", Kaiser, E. T.; Kézdy, F. J., Ed.; Wiley: New York, 1976; Vol. 4, p 1.

(52) Gibian, M. J.; Elliot, D. L.; Kelly, C.; Borge, B.; Kupecz, K. *Z. Naturforsch., B: Anorg. Chem., Org. Chem., Biochem., Biophys., Biol.* **1972**, *27B*, 1016.

(53) von Brdička, R.; Knoblach, E. *Z. Electrochem.* **1941**, *47*, 721.

(54) Jencks, W. P.; Salveson, K. *J. Am. Chem. Soc.* **1971**, *93*, 4433.

(55) Steric hindrance of proton transfer is also likely to apply for the other general catalysts but is not expected to be observed in Brønsted plots. Excluding hydroxide ion, the next largest value of k_{-a1} was only 3 × 10^7 M^{-1} s^{-1} for pyrollidine with **3**. Values for glycine ethyl ester with **6** and triethylene diamine with **4**, 4 × 10^5 and 1 × 10^6 M^{-1} s^{-1}, respectively, were even lower. Thus steric factors much larger than 5–10 must apply to these general bases before deviations from the Brønsted plot would be observable.